CHINESE OPTICS LETTERS

Vol. 22, No. 5 | May 2024

Suppression of nanosecond prepulses from regenerative amplifier and multipass amplifiers in the SULF-1PW laser

Peile Bai (白培乐)[1,2], Zongxin Zhang (张宗昕)[1*], Xinliang Wang (王新亮)[1], Jiayi Qian (钱佳毅)[1], Jiacheng Zhu (朱佳诚)[1], Fenxiang Wu (吴分翔)[1], Jiabing Hu (胡家兵)[1], Xiaojun Yang (杨晓骏)[1], Jiayan Gui (归佳彦)[1], Xiaoming Lu (陆效明)[1], Yanqi Liu (刘彦祺)[1], Yi Xu (许 毅)[1**], Xiaoyan Liang (梁晓燕)[1], Yuxin Leng (冷雨欣)[1***], and Ruxin Li (李儒新)[1]

[1] State Key Laboratory of High Field Laser Physics and CAS Center for Excellence in Ultra-intense Laser Science, Shanghai Institute of Optics and Fine Mechanics (SIOM), Chinese Academy of Sciences (CAS), Shanghai 201800, China

[2] Center of Materials Science and Optoelectronics Engineering, University of Chinese Academy of Sciences, Beijing 100049, China

*Corresponding author: zzx@siom.ac.cn

**Corresponding author: xuyi@siom.ac.cn

***Corresponding author: lengyuxin@mail.siom.ac.cn

Received December 19, 2023 | Accepted January 23, 2024 | Posted Online May 17, 2024

In this research, we report the latest progress in the suppression of nanosecond prepulses from regenerative amplifier and multipass amplifiers in the SULF-1PW laser. The prepulse generated from the Pockels cell (PC) in a regenerative amplifier is delay-shifted by enlarging the distance between the PC and the nearby cavity mirror, and then removed by the extra pulse pickers outside the regenerative amplifier. The prepulses arising from multipass amplifiers are also further suppressed by adopting a novel amplifier configuration and properly rotating the Ti:sapphire crystals. After the optimizations, the temporal contrast on a nanosecond time scale is promoted to be better than a contrast level of 10^{-9}. This research can provide beneficial guidance for the suppression of nanosecond prepulses in the high-peak-power femtosecond laser systems.

Keywords: high-peak-power femtosecond laser; nanosecond prepulses; temporal contrast.
DOI: 10.3788/COL202422.051404

1. Introduction

Since the invention of the chirped pulse amplification (CPA) technique[1], high-peak-power femtosecond laser systems have acquired great progress[2–6]. So far, the highest peak power has reached 10 PW, and the largest focused peak intensity has exceeded 10^{23} W/cm^2[7–9]. For such high-intensity laser facilities, the temporal contrast has become a crucial parameter for laser–matter interactions[10–12]. Since the prepulses or pedestals with intensity over 10^{11} W/cm^2 would inevitably generate preplasma prior to the main pulse in the laser–matter interaction process[13], the methods and techniques to suppress the unwanted prepulses or pedestals while maintaining the focused peak intensity of the main pulse deserve to be taken into consideration. Successful techniques are exerted on the suppression of the amplified spontaneous amplification (ASE) pedestal, including the double-chirped pulse amplification (double-CPA) scheme[14], the saturable absorber[15], the cross-polarized wave generation (XPWG) technique[16], and the optical parametric amplification (OPA) technique[17–19]. Based on the techniques mentioned above, the temporal contrast ratio of ASE can reach 10^{-11}–10^{-12} level in several petawatt (PW)-class lasers. Meanwhile, the "coherent noise" pedestal extending tens of picoseconds around the main pulse can be suppressed by applying a high-order dispersion compensation device and high-quality optical components[20]. The prepulses on picosecond time scale can be eliminated by employing optical components with a small wedge angle. Comparatively, the prepulses on nanosecond time scale (referred to as ns prepulses) have rarely been investigated by researchers.

In a typical CPA laser system, the ns prepulses mainly originate from a regenerative amplifier (RA), a multipass amplifier, and a four-grating compressor[21]. The ns prepulse generated from the four-grating compressor can be suppressed by blocking the zeroth-order diffraction of the gratings. The ns prepulses from the multipass amplifier can be effectively suppressed by adopting a novel amplifier configuration[22]. However, this novel amplifier configuration has only been demonstrated in a four-pass amplifier. For amplifiers with more than four-pass configurations, the scattered noise of the Ti:sapphire needs to be further investigated. As analyzed in Ref. [21], the ns prepulses generated from RA mainly include three types: R1, the leaked ns prepulses due to the limited extinction ratio of the thin-film polarizer (TFP); R2, the ns prepulses from the mismatch on cavity length between the oscillator and the following RA; and R3,

the ns prepulse arising from the Pockels cell (PC) in the RA. The first type of ns prepulse can be suppressed by adding pulse pickers after the RA, while the second type of ns prepulse can be suppressed by adding pulse pickers before the RA. However, the third type of ns prepulse is generally close to the main pulse and is hard to be removed due to the relatively slow rising-edge time of the pulse pickers.

In this research, the work is mainly focused on the investigation and suppression of the third type of prepulse in the RA and the scattered noise in the five-pass Ti:sapphire amplifier. Under the condition that the whole cavity length of the RA is basically unchanged, the distance between the electro-optical crystal located in the PC and the nearby cavity mirror is enlarged. And then the temporally shifted prepulse from the RA can be further suppressed by the subsequent pulse pickers. Meanwhile, applying the optimized multipass amplifier configuration and rotating the Ti:sapphire crystals in the SULF-1PW laser system, the temporal contrast on nanosecond time scale can be promoted to be better than a contrast level of 10^{-9}. The techniques presented here would provide beneficial guidance on the improvement of temporal contrast in high-peak-power femtosecond laser systems. As mentioned in Ref. [21], the ns prepulses were measured mainly by employing a photodiode (ET2030, Electro-Optics Technology) and an oscilloscope (MSO58, Tektronix).

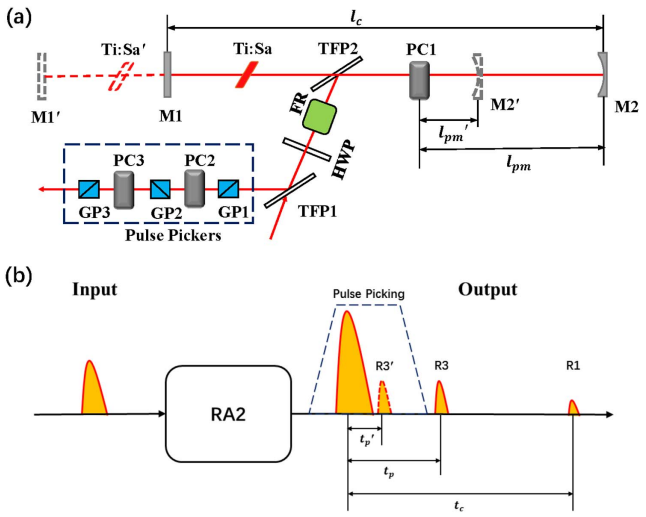

Fig. 1. (a) Scheme of the optimized RA2 in the second CPA stage. M1 and M2 are highly reflective cavity mirrors, while M1′ and M2′ represent their original positions; Ti:Sa and Ti:Sa′ represent the Ti:sapphire crystal and its original position; PC1, PC2, and PC3, Pockels cells; GP1, GP2, and GP3, Glan prisms; TFP1 and TFP2, thin-film polarizers; HWP, half-wave plate; FR, Faraday rotator. (b) Temporal shift of the third type of ns prepulse (R3) from RA2. t_p and t_p' correspond to the distance l_{pm} and l_{pm}', respectively. t_c represents the round-trip time of RA2, corresponding to the cavity length l_c. The dashed trapezium represents the picking gate of the pulse pickers.

2. Optimization of the RA

The SULF-1PW laser system employs a double-CPA structure, which is composed of two CPA stages linked by a nonlinear temporal filter[23]. A commercial Ti:sapphire CPA laser (Astrella, Coherent) serves as the first CPA stage, which includes an oscillator and an RA (RA1). The nonlinear temporal filter composed of XPW and femtosecond OPA supplies relatively clean 100 μJ-level seed laser pulse. In the second CPA stage, the clean seed pulses are temporally expanded to 1.4 ns by an Öffner stretcher and then passed through a pulse picker before RA2, which not only removes the ns prepulse leaked from the first CPA stage, but also eliminates the second type of ns prepulse in RA2. Moreover, cascaded pulse pickers are introduced after RA2 to suppress the first type of ns prepulse from RA2. Then, the third type of ns prepulse becomes the major limitation on the temporal contrast. For the third type of ns prepulse, the distance between the intracavity PC and the nearby cavity mirror should be enlarged so it also can be removed by the cascaded pulse pickers installed after RA2.

As shown in Fig. 1(a), the distance between the internal PC (PC1) and the nearby cavity mirror (M2) is enlarged, while the whole cavity length is basically unchanged to keep the operation stability of RA2. The cavity length of RA2 is ~1.75 m. The positions of the other cavity mirror (M1) and the Ti:sapphire crystal are changed according to the position of M2. The mode sizes at M1 and M2 remain unchanged, 0.98 and 1.08 mm, respectively. The mode size at TFP2 is changed slightly, from 1.03 to 1.00 mm. The modified configuration with unchanged cavity length l_c guarantees the output of the RA without a large adjustment of pump energy and the time synchronization. The pulse pickers after RA2 are composed of two PCs (PC2/PC3) and three Glan prisms (GP1/GP2/GP3). The rise and fall times of the PCs (5046ER, Fastpulse) are ~3 ns, corresponding to the leading and trailing edges of the picking gate shown in Fig. 1(b). The time interval t_p between the main pulse and the third type of ns prepulse (R3) corresponds to the distance l_{pm} between PC1 and M2[21]. To suppress the prepulse R3 by the pulse pickers more effectively, the time interval t_p should be larger than the leading edge of the picking gate. With the distance l_{pm} enlarged by ~0.4 m, the ns prepulse induced by PC1 could be temporally shifted to −4 ns. The prepulse located at −4 ns before the main pulse with a temporal contrast ratio of $\sim 5.1 \times 10^{-7}$ can be detected after the following pulse pickers, as shown in Fig. 2(a). It should be noticed that the −4 ns prepulse still overlaps with the ASE pedestal[15]. Before the RA is optimized, the prepulse would easily be covered by the ASE pedestal[21]. With a fine adjustment on the switching-on time of PC2/PC3, the 4 ns pre-pulse would decay to an undetectable level, as shown in Fig. 2(b).

3. Optimization of the Multipass Amplifiers

As analyzed in Ref. [21], the ns prepulses generated in the multipass amplifiers mainly include two types: BS, the ns prepulses from reflection or backward scattering; and FS, the ns prepulses from forward scattering. The intensity distributions of backward

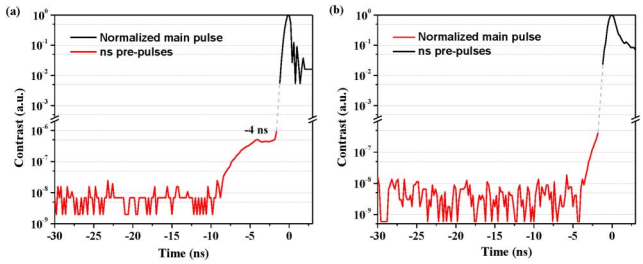

Fig. 2. Detection of ns prepulses after the optimized RA2 and the following pulse pickers. (a) Without adjusting the switching-on time of PC2/PC3, and (b) with an adjustment on the switching-on time of PC2/PC3 for 4 ns delay. The black line represents part of the normalized main pulse, while the red line shows the corresponding ns prepulses.

scattering and forward scattering are angle-dependent with the directions of the reflected and transmitted laser beams[22]. Compared with the forward scattered prepulses, the backward scattered prepulses could be suppressed by optimizing the laser incident angles on the Ti:sapphire crystals, i.e., rotating the Ti:sapphire crystals in the horizontal plane. In this way, the directions of reflected laser beams can be changed to prevent the backward scatterings from entering the optical paths to form ns prepulses. To suppress the forward-scattered prepulses, a novel four-pass amplifier configuration has been demonstrated, which has larger angles between the odd passes or even passes (e.g., the first pass and the third pass) compared with the traditional multipass amplifier configuration[22]. However, amplifiers with more than four-pass configurations would suffer more scattered noise, which makes it more difficult to totally eliminate the ns prepulse induced by the scattering.

The multipass amplifiers in the SULF-1PW laser system originally consisted of a five-pass pre-amplifier, a five-pass power amplifier (Power Amp 1), a three-pass power amplifier (Power Amp 2), and a three-pass final amplifier (Final Amp)[23]. There is no doubt that the scattered noises will increase with the increasing number of passes in the multipass amplifier. To suppress the ns prepulses caused by the scattering, the five-pass Power Amp 1 was modified to be the novel four-pass configuration with slightly reduced beam sizes for both the seed pulses and pump pulses, which can keep the output energy almost the same. Meanwhile, the novel amplifier configuration is also utilized in the three-pass Power Amp 2 and three-pass Final Amp, respectively. By adopting the novel amplifier configuration and properly rotating the Ti:sapphire, both the forward and backward scattering can be effectively suppressed in Power Amp 1, Power Amp 2, and the Final Amp. Then, the five-pass preamplifier would become the major source for the scattering-induced ns prepulse.

The first type of optimized amplifier configuration [shown in Fig. 3(a)] has larger angles between the first/third/fifth passes, while the second type of optimized amplifier configuration [shown in Fig. 3(b)] has a larger angle between the second and fourth passes. The larger angles can let less forward scattering get into the paths of other passes to form ns prepulses. Though the optimized configurations could suppress the

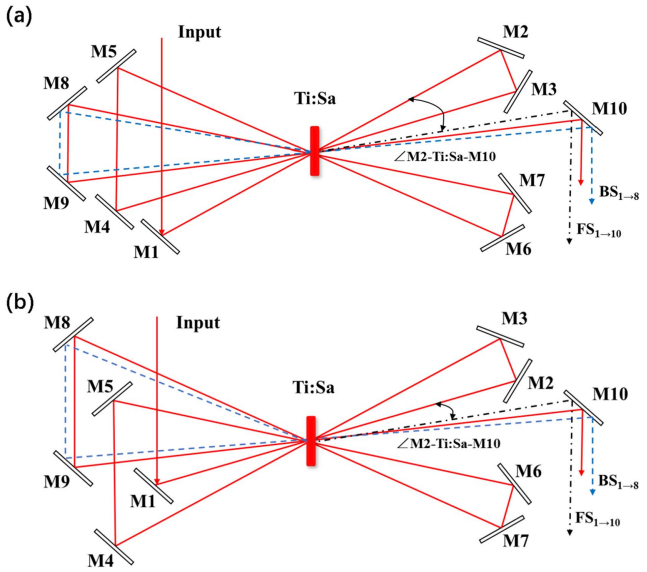

Fig. 3. Optimized five-pass amplifier configurations. (a) With larger angles between the first/third/fifth passes, and (b) with larger angle between the second and fourth passes. M1 to M10 are highly reflective plane mirrors. Ti:Sa represents the Ti:sapphire crystal. The blue dashed line and the black dashed dotted line represent the paths of a backward-scattered prepulse ($BS_{1\to8}$) and a forward-scattered prepulse ($FS_{1\to10}$) generated during the first pass (from M1 to M2). The lines are drawn apart for a better view of the different paths. The intensity of the forward-scattered prepulse $FS_{1\to10}$ is related to the angle between the first pass and the fifth pass (∠M2-Ti:Sa-M10).

intensity level of scattering-induced prepulses, the ns prepulses may still be generated in the optimized five-pass amplifiers, as listed in Table 1. During the first pass (from M1 to M2), two forward-scattered prepulses ($FS_{1\to10}$ and $FS_{1\to6}$) would be generated with the optical paths of M1-Ti:Sa-M10 and M1-Ti:Sa-M6, and two backward-scattered prepulses ($BS_{1\to8}$ and $BS_{1\to4}$) may also be formed with the optical paths of M1-Ti:Sa-M8 and M1-Ti:Sa-M4. During the second pass (from M3 to M4), a forward-scattered prepulse ($FS_{3\to8}$) would be generated with the optical paths of M3-Ti:Sa-M8, and two backward-scattered prepulses ($BS_{3\to6}$ and $BS_{3\to10}$) may also be formed with the optical paths of M3-Ti:Sa-M6 and M3-Ti:Sa-M10. During the third pass (from M5 to M6), a forward-scattered prepulse ($FS_{5\to10}$) and a backward-scattered prepulse ($BS_{5\to8}$) would be generated with the optical paths of M5-Ti:Sa-M10 and M5-Ti:Sa-M8. During the fourth pass (from M7 to M8), a backward-scattered prepulse ($BS_{7\to10}$) would be generated with the optical paths of M7-Ti:Sa-M10.

As seen in Table 1, there are four forward-scattered prepulses ($FS_{1\to10}/FS_{1\to6}/FS_{3\to8}/FS_{5\to10}$) that may be generated in the optimized five-pass amplifier configurations. The intensities of the forward-scattered prepulses ($FS_{1\to6}/FS_{1\to10}/FS_{5\to10}$) are related to the angles between the first/third/fifth passes (∠M2-Ti:Sa-M6, ∠M2-Ti:Sa-M10, and ∠M6-Ti:Sa-M10). The intensity of the forward-scattered prepulse $FS_{3\to8}$ is related to the angle between the second and fourth passes

Table 1. The ns Prepulses May Be Generated in Optimized Five-pass Amplifier Configurations.

Prepulses	Origins	Detailed Paths
$FS_{1\to10}$, $FS_{1\to6}$	Forward scattering/first pass	M1-Ti:Sa-M10, M1-Ti:Sa-M6-M7-Ti:Sa-M8-M9-Ti:Sa-M10
$BS_{1\to8}$, $BS_{1\to4}$	Backward scattering/first pass	M1-Ti:Sa-M8-M9-Ti:Sa-M10, M1-Ti:Sa-M4-M5-Ti:Sa-M6-M7-Ti:Sa-M8-M9-Ti:Sa-M10
$FS_{3\to8}$	Forward scattering/second pass	M3-Ti:Sa-M8-M9-Ti:Sa-M10
$BS_{3\to6}$, $BS_{3\to10}$	Backward scattering/second pass	M3-Ti:Sa-M6-M7-Ti:Sa-M8-M9-Ti:Sa-M10, M3-Ti:Sa-M10
$FS_{5\to10}$	Forward scattering/third pass	M5-Ti:Sa-M10
$BS_{5\to8}$	Backward scattering/third pass	M5-Ti:Sa-M8-M9-Ti:Sa-M10
$BS_{7\to10}$	Backward scattering/fourth pass	M7-Ti:Sa-M10

(∠M4-Ti:Sa-M8). Each of the forward-scattered prepulses has different intensities in the two types of optimized configurations. With a larger corresponding angle, the intensity of the forward-scattered prepulse would be lower. The detailed paths of the prepulses ($FS_{1\to10}$ and $BS_{1\to8}$) are described in Fig. 3 as examples. Comparing the corresponding angles (∠M2-Ti:Sa-M10) in Figs. 3(a) and 3(b), the intensity of the forward-scattered prepulse $FS_{1\to10}$ is lower in the first type of optimized amplifier configuration. The backward-scattered prepulse $BS_{1\to8}$ could be suppressed by rotating the Ti:sapphire crystal to lower the intensity of backward scattering from the crystal to the mirror M8.

To lower the intensities of the forward-scattered prepulses ($FS_{1\to10}$/$FS_{1\to6}$/$FS_{5\to10}$), the amplifier configuration with larger angles (∠M2-Ti:Sa-M6, ∠M2-Ti:Sa-M10, and ∠M6-Ti:Sa-M10) is adopted in the SULF-1PW laser, as shown in Fig. 3(a). For three-pass and four-pass optimized amplifier configurations, M6 and M8 can be used as the output mirrors, respectively. Compared with the amplifier configuration shown in Fig. 3(b), the larger angles (∠M2-Ti:Sa-M10 and ∠M6-Ti:Sa-M10) can make less forward scattering reach M10 to form the prepulses ($FS_{1\to10}$/$FS_{5\to10}$) during the first pass and the third pass, and the larger angle ∠M2-Ti:Sa-M6 can make less forward scattering reach M6 to form the prepulse $FS_{1\to6}$ during the first pass. By optimizing the multipass amplifiers [according to Fig. 3(a)] and properly rotating the Ti:sapphire crystals, no obvious ns prepulses are observed after the second CPA stage at a contrast level of 10^{-9}, as shown in Fig. 4.

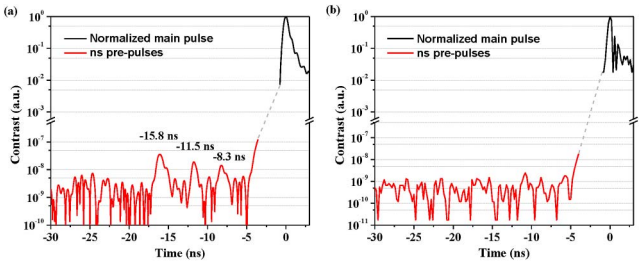

Fig. 4. Detection of ns prepulses after the second CPA stage. (a) With traditional multipass amplifier configurations, and (b) with optimized multipass amplifier configurations. The black line represents part of the normalized main pulse, while the red line shows the corresponding ns prepulses.

4. Conclusion

In conclusion, the ns prepulses in the SULF-1PW laser system are further suppressed. On one side, the distance between the PC and the nearby cavity mirror is enlarged to suppress the ns prepulses arising from the PC in the RA, while keeping the cavity length unchanged. On the other side, the optimized multipass amplifier configuration is employed to suppress the ns prepulses arising from the forward scattering of the Ti:sapphire crystals, while the backward-scattered prepulses could be further suppressed by the rotation of the Ti:sapphire crystals. Based on the above techniques, the temporal contrast on the nanosecond time scale is promoted to be better than a contrast level of 10^{-9} in the SULF-1PW laser. This research can provide beneficial methods for the improvement of the temporal contrast on the nanosecond time scale in the relevant high-peak-power femtosecond laser systems.

Acknowledgements

This work was supported by the National Key R&D Program of China (Nos. 2017YFE0123700 and 2022YFA1604401), the Strategic Priority Research Program of the Chinese Academy of Sciences (No. XDB1603), the National Natural Science Foundation of China (Nos. 61925507 and 62375273), the Program of Shanghai Academic/Technology Research Leader (No. 18XD1404200), and the Shanghai Municipal Science and Technology Major Project (No. 2017SHZDZX02).

References

1. D. Strickland and G. Mourou, "Compression of amplified chirped optical pulses," Opt. Commun. **55**, 447 (1985).
2. T. M. Jeong and J. Lee, "Femtosecond petawatt laser," Ann. Phys. **526**, 157 (2014).

3. C. N. Danson, C. Haefner, J. Bromage, *et al.*, "Petawatt and exawatt class lasers worldwide," High Power Laser Sci. Eng. **7**, e54 (2019).
4. K. Nakamura, H. S. Mao, A. J. Gonsalves, *et al.*, "Diagnostics, control and performance parameters for the BELLA high repetition rate petawatt class laser," IEEE J. Quantum Electron. **53**, 1200121 (2017).
5. J. H. Sung, H. W. Lee, J. Y. Yoo, *et al.*, "4.2 PW, 20 fs Ti:sapphire laser at 0.1 Hz," Opt. Lett. **42**, 2058 (2017).
6. H. Kiriyama, A. S. Pirozhkov, M. Nishiuchi, *et al.*, "High-contrast high-intensity repetitive petawatt laser," Opt. Lett. **43**, 2595 (2018).
7. F. Lureau, G. Matras, O. Chalus, *et al.*, "High-energy hybrid femtosecond laser system demonstrating 2 × 10 PW capability," High Power Laser Sci. Eng. **8**, e43 (2020).
8. W. Q. Li, Z. B. Gan, L. H. Yu, *et al.*, "339 J high-energy Ti:sapphire chirped-pulse amplifier for 10 PW laser facility," Opt. Lett. **43**, 5681 (2018).
9. J. W. Yoon, Y. G. Kim, I. W. Choi, *et al.*, "Realization of laser intensity over 10^{23} W/cm^2," Optica **8**, 630 (2021).
10. X. Chen, X. L. Wang, H. D. Chen, *et al.*, "Delay-shift and asymmetric broadening of pre-pulses by post-pulses in a petawatt laser facility," Appl. Opt. **62**, 7791 (2023).
11. H. D. Chen, X. L. Wang, X. Y. Liu, *et al.*, "Research on the pre-pulses caused by post-pulses in the optical parametric chirped-pulse amplifier," Opt. Express **31**, 40285 (2023).
12. C. Jiang, Z. X. Zhang, H. Dong, *et al.*, "Generation and application of high-contrast laser pulses using plasma mirror in the SULF-1PW beamline," Chin. Opt. Lett. **21**, 043802 (2023).
13. D. Umstadter, "Review of physics and applications of relativistic plasmas driven by ultra-intense lasers," Phys. Plasmas **8**, 1774 (2001).
14. M. P. Kalashnikov, E. Risse, H. Schonnagel, *et al.*, "Double chirped-pulse-amplification laser: a way to clean pulses temporally," Opt. Lett. **30**, 923 (2005).
15. S. Fourmaux, S. Payeur, S. Buffechoux, *et al.*, "Pedestal cleaning for high laser pulse contrast ratio with a 100 TW class laser system," Opt. Express **19**, 8486 (2011).
16. A. Jullien, O. Albert, F. Burgy, *et al.*, "10^{-10} temporal contrast for femtosecond ultraintense lasers by cross-polarized wave generation," Opt. Lett. **30**, 920 (2005).
17. C. Dorrer, I. A. Begishev, A. V. Okishev, *et al.*, "High-contrast optical-parametric amplifier as a front end of high-power laser systems," Opt. Lett. **32**, 2143 (2007).
18. H. D. Chen, X. L. Wang, X. Y. Liu, *et al.*, "High-efficiency, ultra-broadband ns-OPCPA with high temporal contrast based on dual-crystal scheme," Appl. Phys. B **129**, 55 (2023).
19. J. B. Hu, X. L. Wang, X. J. Yang, *et al.*, "Performance improvement of a nonlinear temporal filter by using cascaded femtosecond optical parametric amplification," Opt. Express **29**, 37443 (2021).
20. C. Hooker, Y. X. Tang, O. Chekhlov, *et al.*, "Improving coherent contrast of petawatt laser pulses," Opt. Express **19**, 2193 (2011).
21. P. L. Bai, Z. X. Zhang, X. L. Wang, *et al.*, "Investigation and suppression of pre-pulses on nanosecond time scale in the SULF-1PW laser," Appl. Opt. **61**, 4627 (2022).
22. X. L. Wang, P. L. Bai, Y. Q. Liu, *et al.*, "Suppressing scattering-induced nanosecond pre-pulses in Ti:sapphire multi-pass amplifiers," Opt. Lett. **47**, 5164 (2022).
23. Z. X. Zhang, F. X. Wu, J. B. Hu, *et al.*, "The 1 PW/0.1 Hz laser beamline in SULF facility," High Power Laser Sci. Eng. **8**, e4 (2020).